

# Entanglement and the Kondo effect in serially coupled double quantum dots

A. Ramšak<sup>1,2,a</sup> and J. Mravlje<sup>2</sup>

<sup>1</sup> Faculty of Mathematics and Physics, University of Ljubljana, 1000 Ljubljana, Slovenia

<sup>2</sup> Jožef Stefan Institute, 1000 Ljubljana, Slovenia

Received 26 October 2007 / Received in final form 18 January 2008

Published online 1st March 2008 – © EDP Sciences, Società Italiana di Fisica, Springer-Verlag 2008

**Abstract.** We investigate entanglement between electrons in serially coupled double quantum dots attached to noninteracting leads. In addition to local repulsion we consider the influence of capacitive inter-dot interaction. We show how the competition between extended Kondo and local singlet phases determines the ground state and thereby the entanglement. The results are additionally discussed in connection with the linear conductance through the system.

**PACS.** 73.63.Kv Quantum dots – 03.67.Mn Entanglement production, characterization, and manipulation – 72.15.Qm Scattering mechanisms and Kondo effect

## 1 Introduction

In early days of quantum mechanics the question of entanglement between particles was considered a paradox. Today it has become appreciated that the ability to establish entanglement between qubits in a controlled manner is a crucial ingredient of any quantum information processing system. The interest in such systems is spurred on also by the fact that if a quantum computer were built, it would be capable of tasks impracticable in classical computing [1] as are, e.g., factoring and searching algorithms [2].

In general, it is desirable that the quantum computing hardware meets several criteria as originally proposed by DiVincenzo [3] and include (i) well defined qubits with the feasibility to scale up in number; (ii) the possibility to initialize and manipulate qubit states; (iii) decoherence processes should be minimal that quantum error correction techniques can be applied; and (iv) ability of detecting final qubit states as the outcome of quantum computation. It seems that these criteria for scalable qubits can be met in structures consisting of coupled quantum dots [4,5] which are therefore considered for implementation of quantum computing processes in solid state.

In particular, recent experiments on semiconductor double quantum dot (DQD) devices have shown the evidence of spin entangled states in GaAs based heterostructures [6]. It was shown that vertical-lateral double quantum dots may be useful for implementing two-electron spin entanglement [7] and it was demonstrated that co-

herent manipulation and projective readout is possible in double quantum dot systems [8]. The ability to precisely control the number of electrons by surface gates was also reported [9].

One of the central issues regarding two-qubit operations as the basis for quantum computing algorithms is the creation and the control of qubit pair entanglement in a computing device [1]. The interaction of qubit pairs with their environment is in general a complicated many-body process and its understanding is crucial for experimental solid state realization of qubits in single and double quantum dots [5].

Specifically, the Kondo effect was found to play an important role in single [10] and double quantum dot [11–13] systems and here we report how the Kondo interaction diminishes the entanglement between qubits defined in DQDs even when other sources of decoherence (e.g. phonons) are absent.

The paper is organized as follows. Section 2 introduces the model for coupled qubit pairs – two coupled quantum dots. In Section 3 the entanglement measure relevant for this system is presented. Firstly, spin entanglement for the regime when each of the dots is singly occupied and with weak inter-dot repulsion, and secondly, charge entanglement for the regime, where due to possible strong inter-dot repulsion empty and doubly occupied sites represent dominant contributions to the ground state. The main analysis of the model relies on a numerical approach and is presented in Section 4. Results are summarized in Section 5.

<sup>a</sup> e-mail: [anton.ramsak@fmf.uni-lj.si](mailto:anton.ramsak@fmf.uni-lj.si)

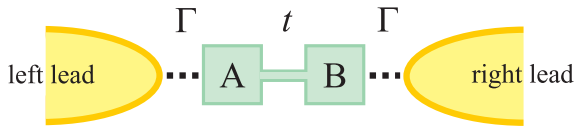


**Fig. 1.** Schematic picture of serial DQD coupled to leads.

## 2 Coupled quantum dots with interaction

One of the simplest examples of solid state qubit realizations is a pair of serially coupled DQDs: a device with the ability to produce entangled pairs that may be extracted using a single-electron turnstile [14]. We model such a DQD using the two-impurity Anderson Hamiltonian

$$H = \sum_{i=A,B} (\epsilon n_i + U n_{i\uparrow} n_{i\downarrow}) + V n_A n_B - t \sum_s (c_{As}^\dagger c_{Bs} + h.c.), \quad (1)$$

where  $c_{is}^\dagger$  creates an electron with spin  $s$  in the dot  $i = A$  or  $i = B$  and  $n_{is} = c_{is}^\dagger c_{is}$  is the number operator. The on-site energies  $\epsilon$  and the Hubbard repulsion  $U$  are taken equal for both dots. The dots are coupled to the left and right noninteracting tight-binding leads with the chemical potential set to the middle of the band of width  $4t_0$ . Each of the dots is coupled to the adjacent lead by hopping  $t'$  and the corresponding hybridization width is  $\Gamma = (t')^2/t_0$ . Schematically this setup is presented in Figure 1. The dots are additionally coupled capacitively by a inter-dot repulsion term  $V n_A n_B$ .

In this paper we concentrate on the low temperature properties of DQD system determined from the ground state. We expand the ground state in the Schönhammer and Gunnarsson projection-operator basis [15,16]  $|\Psi_{\lambda\lambda'ij}\rangle = P_{(\lambda i)} P_{(\lambda' j)} |\hat{0}\rangle$ , which consists of projectors  $P_{\lambda i}$  where  $i \in \{A, B\}$ , - e.g.,  $P_{(0i)} = (1 - n_{i\uparrow})(1 - n_{i\downarrow})$ ,  $P_{(1i)} = \sum_\sigma n_{i\sigma} (1 - n_{i\bar{\sigma}})$ ,  $P_{(2i)} = n_{i\uparrow} n_{i\downarrow}$  - and additional operators involving the operators in leads. We used up to  $\sim 100$  additional combinations of operators consisting of, for example,  $P_{(3ji)} = P_{(0i)} \hat{v}_j P_{(1i)}$ , where  $\hat{v}_{ij}$  denotes the tunneling to/from dot  $i$  to the site  $j$  in the lead. These operators are applied to the state  $|\hat{0}\rangle$ , which is the ground state of the auxiliary noninteracting DQD Hamiltonian of the same form as  $H$ , but with  $U, V = 0$ , renormalized parameters  $\epsilon, t, t' \rightarrow \tilde{\epsilon}, \tilde{t}, \tilde{t}'$  and additional parameter  $\tilde{t}''$  which corresponds to hopping from left dot to right lead and vice versa which although absent in the original Hamiltonian is present in the effective Hamiltonian in some parameter regimes.

The starting point towards the understanding of the ground state of DQDs are the filling properties of isolated DQDs. The first electron is added when  $\epsilon = t$ , and the second when  $\epsilon = -t + J - [(U+V) - |U-V|]/2$ , where  $J = [-|U-V| + \sqrt{(U-V)^2 + 16t^2}]/2$  is the difference between singlet and triplet energies. For  $\epsilon + U/2 + V = 0$  DQD is doubly occupied,  $n = \langle n_A + n_B \rangle = 2$ , and the ground

state is  $\frac{1}{\sqrt{2}}[\alpha(|\uparrow\downarrow\rangle - |\downarrow\uparrow\rangle) + \beta(|20\rangle - |02\rangle)]$ , where  $\alpha/\beta = 4t/(V-U + \sqrt{(U-V)^2 + 16t^2})$ . Here we use notation  $|\uparrow\downarrow\rangle$  corresponding to spin-up and spin-down states on sites A and B, and  $|20\rangle$  to double and zero occupancy of sites A, B. The range of  $\epsilon$  where single occupation is favorable is progressively diminished when  $V \neq U$ . For large  $t$  or at (and near)  $V = U$  the molecular bonding and antibonding orbitals are formed as is seen here from  $\alpha \sim \beta$ .

When DQDs are attached to the leads the low temperature physics is to the large extent the same as that of the two-impurity Kondo problem studied by Jones, Varma and Wilkins two decades ago [17,18]. There two impurities form either two Kondo singlets with delocalized electrons or bind into a local spin-singlet state which is virtually decoupled from delocalized electrons. The crossover between the regimes is determined by the relative values of the exchange magnetic energy  $J$  and twice the Kondo condensation energy, of order the Kondo temperature given by the Haldane formula,  $T_K = \sqrt{UF}/2 \exp(|\epsilon| |\epsilon + U| / 2FU)$ . Such results were obtained by the analysis of a two-impurity Anderson model by means of slave-boson formalism [19–23], numerical renormalization group [24–26] or present formalism [26,27]. Resembling behavior was found also in particular regimes of triple quantum dot systems [28], and DQDs in side coupled [29] and parallel [30] configurations. As a side note we remark that the slave boson saddle-point approximation is equivalent to the Schönhammer-Gunnarsson method applied with the minimal set of operators [31], which for the present case of stronger coupling would not give converged results. The advantage of the present formalism over the numerical renormalization group approach is mainly diminished numerical effort in the regimes of small and moderate interaction strengths which are considered here. Additionally, in the present approach the interpretation of the results and the calculation of various local correlation functions can be more direct, because the ground state wave function is explicitly available.

## 3 Entanglement

### 3.1 Spin entanglement

Quantum entanglement as a physical resource was first defined for two distinguishable particles in a pure state through von Neumann entropy and concurrence [32–35]. However, amongst the realistic systems of major physical interest, electron-qubits have the potential for a much richer variety of entanglement measure choices due to both their charge and spin degrees of freedom. In systems of identical particles, for example, generalizations are needed to define an appropriate entanglement measure which adequately deals with multiple occupancy states [36–39].

When entanglement is quantified in fermionic systems the measure must also account for the effect of exchange [40] as well as of mutual electron repulsion. In lattice fermion models entanglement is sensitive to the interplay between charge hopping and the avoidance of

double occupancy due to the Hubbard repulsion, which results in an effective Heisenberg interaction between adjacent spins [41]. Entangled fermionic qubits can be created with electron-hole pairs in a Fermi sea [42] and in the scattering of two distinguishable particles [43]. A spin-independent scheme for detecting orbital entanglement of two-quasiparticle excitations of a mesoscopic normal-superconductor system was also proposed recently [44].

For two distinguishable particles A and B, described with single spin- $\frac{1}{2}$  (or pseudo spin) states  $s = \uparrow$  or  $\downarrow$  and in a pure state  $|\Psi_{AB}\rangle = \sum_{ss'} \alpha_{ss'} |s\rangle_A |s'\rangle_B$  concurrence as a measure of entanglement is given by [33]

$$C_0 = 2|\alpha_{\uparrow\uparrow}\alpha_{\downarrow\downarrow} - \alpha_{\uparrow\downarrow}\alpha_{\downarrow\uparrow}|. \quad (2)$$

Two qubits are completely entangled,  $C_0 = 1$ , if they are in one of the Bell states [32], e.g., singlet  $|\Psi_{AB}\rangle \propto |\uparrow\downarrow\rangle - |\downarrow\uparrow\rangle$ .

A qubit pair represented by two electrons in DQDs and in the contact with the leads acting as a fermionic bath can not be described by a pure state and entanglement can not be related to the concurrence given with the Wootters formula equation (2) relevant for pure states. In the case of mixed states describing qubit pairs concurrence is related to the reduced density matrix of the DQD subsystem [35,45,46], where for systems that are axially symmetric in spin space the concurrence may conveniently be given in the closed form [47],

$$\begin{aligned} C_0 &= \max(0, C_{\uparrow\downarrow}, C_{\parallel}), \\ C_{\uparrow\downarrow} &= 2|\langle S_A^+ S_B^- \rangle| - 2\sqrt{\langle P_A^\uparrow P_B^\uparrow \rangle \langle P_A^\downarrow P_B^\downarrow \rangle}, \\ C_{\parallel} &= 2|\langle S_A^+ S_B^+ \rangle| - 2\sqrt{\langle P_A^\uparrow P_B^\downarrow \rangle \langle P_A^\downarrow P_B^\uparrow \rangle}, \end{aligned} \quad (3)$$

where  $S_i^+ = (S_i^-)^\dagger = c_{i\uparrow}^\dagger c_{i\downarrow}$  is the electron spin raising operator for dot  $i = A$  or  $B$  and  $P_i^s = n_{is}(1 - n_{i,-s})$  is the projection operator onto the subspace where dot  $i$  is occupied by one electron with spin  $s$ .

In the derivation of concurrence formula equation (3) the reduced density matrix was obtained by projecting onto four local spin states of  $|\uparrow\rangle_A, |\downarrow\rangle_A, |\uparrow\rangle_B$ , and  $|\downarrow\rangle_B$ , corresponding to *singly* occupied DQD sites A and B, respectively. If  $t/U$  is not small the electrons tunnel between the dots and charge fluctuations introduce additional states with zero or double occupancy of individual dots [36,41]. As pointed out by Zanardi [41] in the case of simple Hubbard dimer the entanglement is not related only to spin but also to charge degrees of freedom which emerge when repulsion between electrons is weak or moderate.

For systems with strong electron-electron repulsion, charge fluctuations are suppressed and the states with single occupancy – the spin-qubits – dominate: the concept of spin-entanglement quantified with concurrence can still be applied. We use spin-projected density matrix and consider only entanglement corresponding to *spin* degrees of freedom. Due to doubly (or zero) occupied states arising from charge fluctuation on the dots (caused by tunneling between the dots A and B or due to the exchange with

the electrons in the leads), the reduced density matrix has to be renormalized. The probability that at the measurement of entanglement there is precisely one electron on each of the dots is less than unity,  $P_{11} < 1$ , and the spin-concurrence is then given with

$$C = C_0/P_{11}, \quad (4)$$

where  $P_{11} = P_{\uparrow\downarrow} + P_{\parallel}$ , and  $P_{\uparrow\downarrow} = \langle P_A^\uparrow P_B^\downarrow + P_A^\downarrow P_B^\uparrow \rangle$ ,  $P_{\parallel} = \langle P_A^\uparrow P_B^\uparrow + P_A^\downarrow P_B^\downarrow \rangle$  are probabilities for antiparallel and parallel spin alignment, respectively. Such procedure corresponds to the measurement apparatus which would only discern spins and ignore all cases whenever no electron, or a electron pair would appear at one of the detectors at sites A or B.

### 3.2 Charge (isospin) entanglement

At half-filling in the ground state of two isolated impurities coupled by a capacitive (but not tunneling) term  $V = U$ , 4 ‘spin states’  $|\sigma_1\sigma_2\rangle$  and 2 ‘charge states’  $|20\rangle, |02\rangle$  are degenerate. By introducing the pseudospin operator [48]  $\tilde{T}^i = 1/2 \sum_{l=A,B} \sum_{\sigma} c_{l\sigma}^\dagger \tau_{ll}^i c_{l\sigma}$ , where  $\tau^i$  are the Pauli matrices, and the combined spin-pseudospin operators  $W^{ij} = S^i \tilde{T}^j$ , the Hamiltonian is evidently SU(4) symmetric. As long as the SU(4) symmetry breaking terms are small enough (e.g., tunneling  $t \rightarrow 0$ ) the ground state of such DQDs attached to the leads remains close to an SU(4) symmetric state with ‘spin’ screened by the electrons in the leads [27]. The same symmetry group due to additional orbital degree of freedom occurs also in single impurity (quantum dot) formed in carbon nanotubes [50,51].

If  $V \gg U$  charge states dominate and in this case *charge concurrence* can be defined in a direct analogy with the previous spin case. In equation (3) one just has to replace the spin operators with their corresponding isospin counterparts, e.g.,  $S_\lambda^- = c_{\lambda\downarrow}^\dagger c_{\lambda\uparrow} = (S_\lambda^+)^\dagger \rightarrow T_\lambda^- = c_{\lambda\uparrow} c_{\lambda\downarrow} = (T_\lambda^+)^\dagger$  for sites  $\lambda = A, B$  and  $S_\lambda^z = (n_{\lambda\uparrow} - n_{\lambda\downarrow})/2 \rightarrow T_\lambda^z = (n_\lambda - 1)/2$ . If the probability for spin states is significant, appropriate renormalization to charge states is analogous to equation (4), but with corresponding isospin operators. The density matrix is here renormalized with the probability  $P_{20}$  that precisely  $n_{A,B} = 2$  and  $n_{B,A} = 0$  electrons occupy individual dots (corresponding to apparatus which only measures occurrence or absence of pairs at each of its detectors).

## 4 Numerical results

### 4.1 Concurrence

We here present the results for zero temperature (ground state) concurrence of a qubit pair in DQDs in the absence of magnetic field. Temperature dependence of concurrence for the case of  $V = 0$  is given in reference [26].

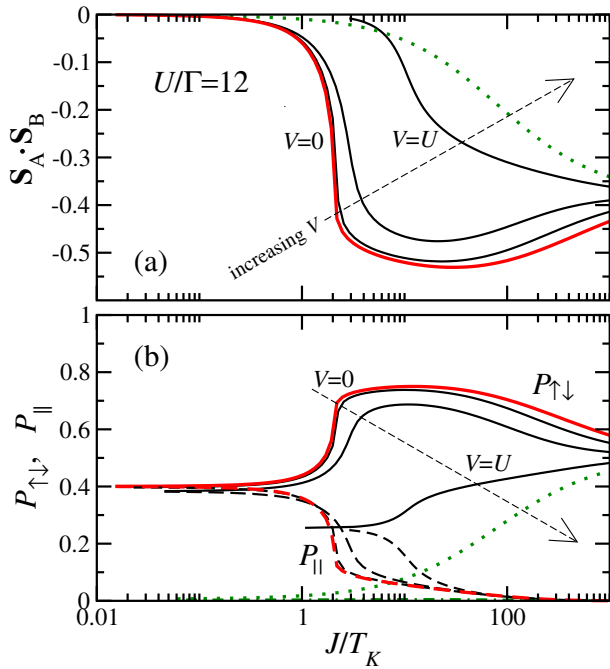


**Fig. 2.** (a) Spin-spin correlation for  $V/U = 0, 1/3, 2/3, 1$  (full lines) and  $V/U = 5/4$  (dotted) for  $U/\Gamma = 12$ ,  $\Gamma/t_0 = 0.1$ . (b) Probabilities for parallel (lower curves - dashed) and anti-parallel (upper curves - full) spins of electrons in the DQD for  $V/U$  ratios as in (a). Note that the probability for parallel spins for  $V/U = 5/4$  is almost zero (dashed-dotted), while  $P_{\uparrow\downarrow} < 1/2$  for  $J/T_K < 1000$  (dotted); the probabilities do not sum to 1. The deficiency (which goes to zero as  $U \rightarrow \infty$ ) is due to states with double particle (or hole) occupancy on at least one dot.

Expectation values  $\langle \dots \rangle$  in the concurrence formula equation (3) are now calculated using the ground state therefore  $\langle S_A^+ S_B^+ \rangle = 0$  and  $C_{\parallel} < 0$ . We consider the particle-hole symmetry point with  $n = 2$  and  $\epsilon + U/2 + V = 0$ .

Qualitatively, the concurrence is significant whenever enhanced spin-spin correlations indicate inter-dot singlet formation. As shown in Figure 2a for  $U/\Gamma = 12$  and  $\Gamma/t_0 = 0.1$ , the correlation function  $\langle S_A S_B \rangle$  tends to  $-3/4$  for  $J$  large enough to suppress the formation of Kondo singlets, but still  $J/U \ll 1$ , that local charge fluctuations are sufficiently suppressed. In particular, the local dot-dot singlet is formed whenever singlet-triplet splitting superexchange energy  $J > J_c \sim 2T_K$ . With increasing  $V \rightarrow U$ , and above  $U$ , the probability for singly occupied spin states,  $P_{11} = P_{\uparrow\downarrow} + P_{\parallel}$  is significantly reduced, Figures 2b and 3, which also leads to reduced spin-spin correlation, Figure 2a. In this limit the concept involving isospin entanglement can be applied (not shown here).

Concurrence, corresponding to the correlation function from Figures 2a, 2b is presented in Figure 3 for various values of  $V$ . As discussed above, in the  $V = 0$  case  $C$  is zero for  $J$  below  $\sim 2T_K$  due to the Kondo effect, which leads to entanglement between localized and conducting electrons [52] instead of the A-B qubit pair entanglement. On the other hand, for  $V \sim U$  the concurrence rises only at  $J \sim 10T_K$  because the Kondo temperature rises near

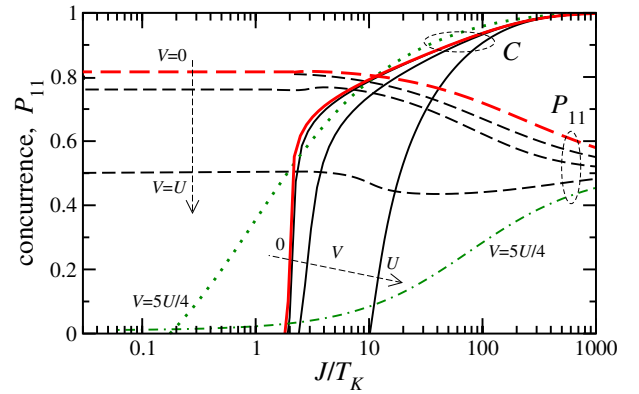


**Fig. 3.** Concurrence (full curves) and single particular dot occupation probability  $P_{11}$  (dashed) for  $V/U = 0, 1/3, 2/3, 1$ . For  $V/U = 5/4$  the concurrence and  $P_{11}$  are plotted dotted and dashed-dotted, respectively. Parameters are as in Figure 2.

the point of  $SU(4)$  symmetry due to the increased degeneracy (note that in our notation  $T_K$  corresponds to the ordinary  $SU(2)$  Kondo regime and is not a function of  $V$ ). In finite magnetic field irrespectively of temperature the concurrence abruptly tends to zero for  $B > J$  (not shown here) [53].

The entanglement between qubits quantified by concurrence is small in the regime where the Kondo effect determines the ground state (left side of Fig. 3). The Kondo screening transfers the entanglement between localized electrons to the mutual entanglement of localized and the conducting electrons [52]. For  $V \sim U$  the Kondo temperature is enhanced and the corresponding Kondo ground state is competitive towards the localized singlet state. For  $V > U + T_K$  the Kondo screening is inhibited [49] and the concurrence is increased (Fig. 3, dotted). However, the probability for singly occupied states (Fig. 3, dashed-dotted) is small. In this regime the charge-charge entanglement is large for all  $J$  as there is no competing ground state – no Kondo effect occurs here and the isospin entanglement in this regime would be similar to that of the isolated dimer (not shown here).

## 4.2 Conductance

One of the most directly measurable properties of DQDs is the linear conductance. We calculate the zero temperature conductance using the sine formula (SF) [54–56],  $G = G_0 \sin^2[(E_+ - E_-)/4t_0L]$ , where  $G_0 = 2e^2/h$  and  $E_{\pm}$  are the ground state energies of a large auxiliary ring consisting of  $L$  non-interacting sites and an embedded DQD, with periodic and anti-periodic boundary conditions, respectively. Alternatively conductance can be obtained also from the Green's function (GF) corresponding to the effective noninteracting Hamiltonian  $\tilde{H}$  with effective parameters [54,57]. The advantage of the former method is better convergence in the strong coupling regime, however, the accuracy of the SF method depends only on the accuracy of the ground-state energy and is therefore in some cases

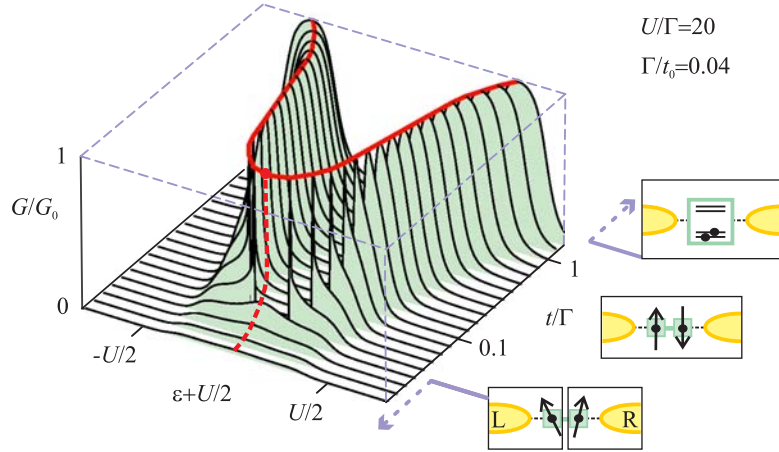


**Fig. 4.** Conductance of DQD as a function of gate voltage and inter-dot tunneling rate for  $U/\Gamma = 20$ ,  $\Gamma/t_0 = 0.04$ . Pictograms indicate dominant ground state regimes: molecular orbital Kondo effect, local spin-singlet formation and two separate Kondo effects.

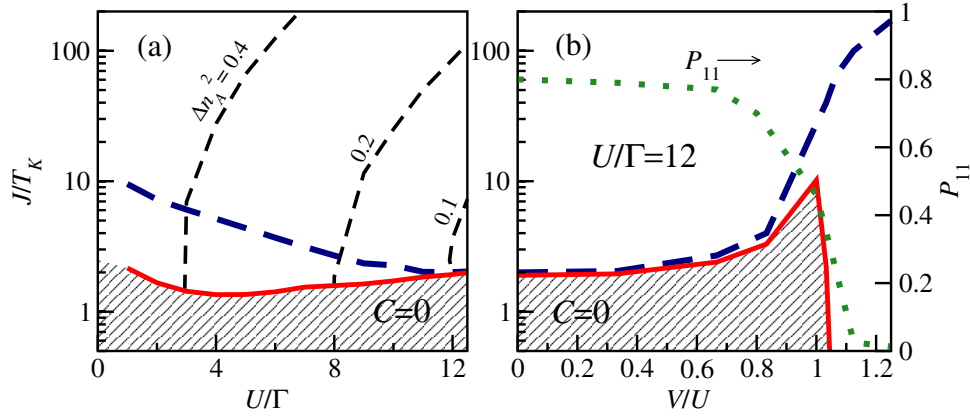


**Fig. 5.** (a) Charge fluctuations (short-dashed),  $\mathbf{S}_A \mathbf{S}_B = -1/4$  (long-dashed) and  $C = 0$  (full) in the  $(U/\Gamma, J/T_K)$  plane. (b)  $\mathbf{S}_A \mathbf{S}_B = -1/4$  (long-dashed) and  $C = 0$  (full) in the  $(V/U, J/T_K)$  plane.  $P_{11}$  is shown with dotted line (right scale).

more robust. By comparing results of both methods we checked for the consistency and the convergence.

The conductance as a function of interdot hopping  $t$  and  $\epsilon + U/2$  in the absence of interdot repulsion,  $V = 0$ , is presented in Figure 4. The Hubbard repulsion is set to  $U/\Gamma = 20$  and hybridization to  $\Gamma/t_0 = 0.04$ . As in the previous Section three different regimes of  $t$  correspondingly reflect in the results for conductance. For large  $t/\Gamma > 1$  (but with  $\Gamma/U \ll 1$ ) the DQD is in molecular-orbital Kondo regime when occupancy is odd, i.e.,  $n \sim 1, 3$ . Typical Kondo conductance plateau of width  $\sim U/2$  is developed around bonding (and anti-bonding) molecular orbital level  $\pm t$ . These two unitary conductance regions with reducing  $t$  become progressively sharper when we enter  $t/U \ll 1$  regime. There the description of DQD in terms of bonding/anti-bonding orbitals should be replaced with local picture. Due to strong electron-electron repulsion local charge fluctuations are suppressed at the point of particle-hole symmetry with  $n = 2$  and  $\epsilon + U/2 = 0$ . Thick full line corresponds to points of  $G = G_0$  and there exists some

critical  $t_c$  where two conductance peaks merge (bullet) and for  $t < t_c$  conductance is less than  $G_0$  (dashed line). The corresponding critical superexchange interaction is of the order of Kondo temperature as before,  $J_c \sim 2T_K$ . As discussed above, in this regime each of the dots undergoes the Kondo effect where local moment is screened by conducting electrons in the adjacent lead and left – right sides of the system become decoupled which leads to vanishing  $A \rightarrow B$  conductance as  $G \propto (t/\Gamma)^2$  [19].

## 5 Summary

The main results concerning entanglement of qubit pairs in serially coupled double quantum dots are extracted in Figure 5. The charge fluctuations  $\Delta n_A^2 = \langle n_A^2 \rangle - \langle n_A \rangle^2$ , contour plot in Figure 5a, are suppressed for sufficiently large repulsion, e.g.,  $U/\Gamma > 10$ . In this limit and in vanishing magnetic field, the DQD can be described in terms of the Werner states [58] and becomes similar to

recently studied problem of entanglement of two Kondo spin impurities embedded in a conduction band [59]. In this case,  $C_{\uparrow\downarrow} \sim 2(-\langle \mathbf{S}_A \mathbf{S}_B \rangle - \frac{1}{4}) \sim P_{\uparrow\downarrow} - 2P_{\parallel}$  for  $C_{\uparrow\downarrow} \geq 0$ . For large  $U/\Gamma$ , where the charge fluctuations vanish, the  $\langle \mathbf{S}_A \mathbf{S}_B \rangle = -\frac{1}{4}$  line (dashed line) progressively merges with the  $C = 0$  boundary line (full).

In Figure 5b phase diagram with fixed  $U/\Gamma = 12$  and corresponding to Figure 5a presents  $V/U$  dependence of  $C = 0$  boundary line (full) in comparison with the  $\langle \mathbf{S}_A \mathbf{S}_B \rangle = -\frac{1}{4}$  line (dashed). With  $V$  exceeding  $U$  the probability for well defined spin-qubit pairs in DQD,  $P_{11}$ , rapidly decreases which means that states with doubly occupied or empty individual dots dominate. In this regime  $C = 0$  line is pushed to much lower  $J/T_K$ . For  $V > U$  the probability  $P_{11}$  becomes progressively negligible giving more meaning to considering charge (isospin) entanglement instead. It should be noted, however, that in realistic DQD systems intersite repulsion  $V$  is in general weaker compared to  $U$  and that this regime would not be easily reached experimentally. One possibility, where  $V$ -interaction could dominate, are systems with strong local electron-phonon interactions which may significantly renormalize local  $U$  [60] without affecting capacitive interaction  $V$ .

To conclude, we have found generic behavior of spin-entanglement of an electron pair in serially coupled double quantum dots. On the one hand, we have shown quantitatively that making the spin-spin exchange coupling  $J$  large by increasing tunneling  $t$ , leads to enhanced charge fluctuations, whilst on the other, at small magnetic interactions  $J < J_c$  entanglement is suppressed as the DQD system undergoes the Kondo effect. Various regimes are explained and supported with typical numerical examples.

We thank T. Rejec for his GS code and suggestions. We acknowledge J. Bonča and R. Žitko for useful discussions. We also acknowledge support from the Slovenian Research Agency under contract PI-0044.

## References

- M.A. Nielsen, I.A. Chuang, *Quantum Information and Quantum Computation* (Cambridge University Press, Cambridge, 2001); N.D. Mermin, *Quantum Computer Science: An Introduction* (Cambridge University Press, Cambridge, 2007)
- P.W. Shor, Proc. 35th Annu. Symp. Foundations of Computer Science, 124, IEEE Computer Society Press, Los Alamitos, 1994
- D.P. DiVincenzo, *Mesoscopic Electron Transport, NATO Advanced Studies Institute, Series E: Applied Science*, edited by L. Kouwenhoven, G. Schön, L. Sohn (Kluwer Academic, Dordrecht, 1997) arXiv:cond-mat/9612126
- D.P. DiVincenzo, Science **309**, 2173 (2005)
- W.A. Coish, D. Loss, arXiv:cond-mat/0603444
- J.C. Chen, A.M. Chang, M.R. Melloch, Phys. Rev. Lett. **92**, 176801 (2004)
- T. Hatano, M. Stopa, S. Tarucha, Science **309**, 268 (2005)
- J.R. Petta, A.C. Johnson, J.M. Taylor, E.A. Laird, A. Yacoby, M.D. Lukin, C.M. Marcus, M.P. Hanson, A.C. Gossard, Science **309**, 2180 (2005)
- J.M. Elzerman, R. Hanson, J.S. Greidanus, L.H. Willems van Beveren, S.D. Franceschi, L.M.K. Vandersypen, S. Tarucha, L.P. Kouwenhoven, Phys. Rev. B **67**, 161308 (2003), J.M. Elzerman, R. Hanson, J.S. Greidanus, L.H. Willems van Beveren, S.D. Franceschi, L.M.K. Vandersypen, S. Tarucha, L.P. Kouwenhoven, Appl. Phys. Lett. **65**, 1012 (1994)
- D. Goldhaber-Gordon, H. Shtrikman, D. Mahalu, D. Abusch Magder, U. Meirav, M.A. Kastner, Nature **391**, 156 (1998)
- H. Jeong, A.M. Chang, M.R. Melloch, Science **293**, 2221 (2001)
- U. Wilhelm, J. Schmid, J. Weis, K.v. Klitzing, Physica E **14**, 385 (2002)
- A.W. Holleitner, R.H. Blick, A.K. Httel, K. Eberl, J.P. Kotthaus, Science **297**, 70 (2002)
- X. Hu, S. DasSarma, Phys. Rev. B **69**, 115312 (2004)
- K. Schönhammer, Phys. Rev. B **13**, 4336 (1976)
- O. Gunnarsson, K. Schönhammer, Phys. Rev. B **31**, 4815 (1985)
- B.A. Jones, C.M. Varma, J.W. Wilkins, Phys. Rev. Lett. **61**, 125 (1988)
- B.A. Jones, C.M. Varma, Phys. Rev. B **40**, 324 (1989)
- T. Aono, M. Eto, K. Kawamura, J. Phys. Soc. Jpn. **67**, 1860 (1998)
- A. Georges, Y. Meir, Phys. Rev. Lett. **82**, 3508 (1999)
- R. Aguado, D.C. Langreth, Phys. Rev. Lett. **85**, 1946 (2000)
- T. Aono, M. Eto, Phys. Rev. B **63**, 125327 (2001)
- R. Lopez, R. Aguado, G. Platero, Phys. Rev. Lett. **89**, 136802 (2002)
- W. Izumida, O. Sakai, Y. Shimizu, Physica B **259**, 215 (1999)
- W. Izumida, O. Sakai, Phys. Rev. B **62**, 10260 (2000)
- A. Ramšak, J. Mravlje, R. Žitko, J. Bonča, Phys. Rev. B **74**, 241305 (R) (2006)
- J. Mravlje, A. Ramšak, T. Rejec, Phys. Rev. B **73**, 241305 (2006)
- R. Žitko, J. Bonča, A. Ramšak, T. Rejec, Phys. Rev. B **73**, 153307 (2006)
- R. Žitko, J. Bonča, Phys. Rev. B **73**, 035332 (2006)
- R. Žitko, J. Bonča, Phys. Rev. B **74**, 045312 (2006)
- K. Schönhammer, Phys. Rev. B **42**, 2591 (1990)
- C.H. Bennett, H.J. Bernstein, S. Popescu, B. Schumacher, Phys. Rev. A **53**, 2046 (1996); C.H. Bennett, D.P. DiVincenzo, J.A. Smolin, W.K. Wootters, C.H. Bennett, H.J. Bernstein, S. Popescu, B. Schumacher, Phys. Rev. A **54**, 3824 (1996)
- S. Hill, W.K. Wootters, Phys. Rev. Lett. **78**, 5022 (1997)
- V. Vedral, M.B. Plenio, M.A. Rippin, P.L. Knight, Phys. Rev. Lett. **78**, 2275 (1997)
- W.K. Wootters, Phys. Rev. Lett. **80**, 2245 (1998)
- J. Schliemann, D. Loss, A.H. MacDonald, Phys. Rev. B **63**, 085311 (2001); J. Schliemann, J.I. Cirac, M. Kuš, M. Lewenstein, D. Loss, Phys. Rev. A **64**, 022303 (2001)
- G.C. Ghirardi, L. Marinatto, Phys. Rev. A **70**, 012109 (2004)
- K. Eckert, J. Schliemann, G. Brus, M. Lewenstein, Ann. Phys. **299**, 88 (2002)

39. J.R. Gittings, A.J. Fisher, *Phys. Rev. A* **66** 032305 (2002)
40. V. Vedral, *Cent. Eur. J. Phys.* **2**, 289 (2003); D. Cavalcanti, M.F. Santos, M.O. TerraCunha, C. Lunkes, V. Vedral, *Phys. Rev. A* **72**, 062307 (2005)
41. P. Zanardi, *Phys. Rev. A* **65**, 042101 (2002)
42. C.W.J. Beenakker, M. Titov, B. Trauzettel, *Phys. Rev. Lett.* **94**, 186804 (2005); C.W.J. Beenakker, [arXiv:cond-mat/0508488](https://arxiv.org/abs/cond-mat/0508488)
43. A. Bertoni, *J. Com. Electron.* **2**, 291 (2003); P. Bordone, A. Bertoni, C. Jacoboni, *J. Com. Electron.* **3**, 407 (2004)
44. P. Samuelsson, E.V. Sukhorukov, M. Büttiker, *Phys. Rev. Lett.* **91**, 157002 (2003); P. Samuelsson, E.V. Sukhorukov, M. Büttiker, *New J. Phys.* **7**, 176 (2005)
45. A. Osterloh, L. Amico, G. Falci, R. Fazio, *Nature* **416**, 608 (2002)
46. O.F. Syljuåsen, *Phys. Rev. A* **68**, 060301(R) (2003)
47. A. Ramšak, I. Sega, J.H. Jefferson *Phys. Rev. A* **74**, 010304 (2006)
48. L.D. Leo, Michele Fabrizio, *Phys. Rev. B* **69**, 245114 (2004)
49. M.R. Galpin, D.E. Logan, H.R. Krishnamurthy, *Phys. Rev. Lett.* **94**, 1864406 (2005)
50. P. Jarrilo-Herrero et al., *Nature* **434**, 484 (2005)
51. M.S. Choi, R. Lopez, R. Aguado, *Phys. Rev. Lett.* **95**, 067204 (2005)
52. A. Rycerz, *Eur. Phys. J. B* **52**, 291 (2006); S. Oh, J. Kim, *Phys. Rev. B* **73**, 052407 (2006)
53. R. Žitko, J. Bonča, A. Ramšak, unpublished
54. T. Rejec, A. Ramšak, *Phys. Rev. B* **68**, 035342 (2003)
55. T. Rejec, A. Ramšak, *Phys. Rev. B* **68**, 033306 (2003)
56. A. Ramšak, J. Bonča, T. Rejec, [arXiv:cond-mat/0407590](https://arxiv.org/abs/cond-mat/0407590)
57. J. Mravlje, A. Ramšak, T. Rejec *Phys. Rev. B* **74**, 205320 (2006)
58. R.F. Werner, *Phys. Rev. A* **40**, 4277 (1989)
59. S.Y. Cho, R.H. McKenzie, *Phys. Rev. A* **73**, 012109 (2006)
60. J. Mravlje, A. Ramšak, T. Rejec, *Phys. Rev. B* **72**, 121403(R) (2005)